IEEE Trans. Pattern Anal. and Machine Intell., vol. 15, pp. 1202–1208, Nov. 1993.

Direct Estimation of Shape from Texture

Jonas Gårding
Computational Vision and Active Perception Laboratory (CVAP)
Department of Numerical Analysis and Computing Science
Royal Institute of Technology, S-100 44 Stockholm, Sweden
Email: jonasg@bion.kth.se

August 25, 1992

Abstract

In [12], Witkin proposed a maximum likelihood (ML) estimator of surface orientation based on the observed directional bias of projected texture elements. However, a drawback of this procedure is that the estimate is only defined indirectly in terms of a set of non-linear equations. In this paper we propose an alternative method, which allows an estimate of the surface orientation to be computed *directly* in a single step from certain simple statistics of the image data. We also show that this direct estimate allows Witkin's ML estimate to be computed to within 0.05° in only two or three iterative steps. The performance of the new estimator is demonstrated experimentally and compared to that of the ML estimator, using both synthetic data and real gray-level images.

Index Terms: Shape from texture, surface orientation, foreshortening, isotropy, distributions on the circle, maximum likelihood, method of moments

1 Introduction

Although direct information about depth and three-dimensional structure is available from binocular and dynamical visual cues, static monocular images can also provide important constraints on the structure of the scene. The use of *projective distortion of surface texture* as a cue to surface shape was first studied by Gibson [9], who emphasized the role of "texture gradients", i.e., the rate of change in the retinal array of the projective distortion of the surface pattern.

However, texture gradients are not the only possible cues of this type. Witkin [12] pointed out that the *foreshortening* effect can also be a cue to surface orientation. The term foreshortening refers to the fact that the image of a slanted pattern is systematically compressed in the direction of slant; for example, the image of a slanted circle is an ellipse. Whereas texture gradients are primarily due to *perspective* effects, the foreshortening effect can also be observed in *orthographic* projection of a planar pattern. (See [8] for a general analysis of the geometric information content of various shape-from-texture cues.)

Witkin [12] used the foreshortening effect to derive an elegant maximum likelihood (ML) estimator for the surface orientation, based on the simplifying assumptions of orthographic projection and independent needle-like texture elements with orientation sampled from a uniform distribution. However, the ML estimate requires a set of non-linear equations to be solved, and the computational procedure Witkin suggested was fairly inefficient. Davis *et al* [5] later corrected some minor errors in Witkin's analysis, and derived a more efficient algorithm which finds a good approximation of the ML estimate. Blake and Marinos [1] showed that both Witkin's ML estimator and the maximum compactness estimator of Brady and Yuille [2] can be expressed in terms of moment tensors. They also proposed an iterative algorithm for computing the ML estimate, and presented a detailed statistical analysis of the estimator.

Alternative approaches which ease the rather restrictive assumptions behind the ML estimator have also been suggested, e.g. by Kanatani [10] and Gårding [7]. However, in this paper we shall not be concerned with these more general approaches. Instead, we retain Witkin's original assumptions, and show that under these conditions it is possible to obtain a *direct* estimate of surface orientation expressed in closed form, using only simple statistics of the orientation of texture elements in the image.

This estimator, which is based on the method of moments (MM), can either be used as an estimator in its own right, or as an initial approximation in an efficient iterative technique for finding the ML estimate.

The structure of the paper is the following. In Section 2 we briefly review Witkin's ML estimator. In Section 3 we introduce some useful statistical concepts, and in Section 4 these are applied to derive the new MM estimator. An efficient technique for numerical computation of the ML estimate is described in Section 5. In Section 6 some experimental results are shown, allowing the performance of the MM and ML estimators to be compared.

2 The ML estimator

It is useful to start with a brief review of Witkin's ML estimator [12], since the work we will describe here builds on precisely the same models of surface geometry and texture.

As shown in Fig. 1, the geometric setting is a planar surface S projected orthographically

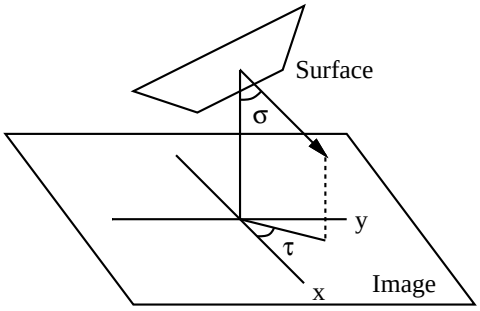

Figure 1: Planar surface model.

onto the image plane I. The orientation of the surface can be represented in a number of ways, but a particularly convenient choice of parameters is (σ, τ), where $\sigma \in [0, \pi]$ is the *slant*, and $\tau \in [0, 2\pi]$ is the *tilt*. The slant is the angle between the optic axis and the surface normal, and the tilt is the angle between the parallel projection of the surface normal onto the image plane and the x-axis in the image. (A third parameter necessary to determine the position of the plane in three-space is the perpendicular distance from the origin, but this parameter never enters into the computations since orthographic projection is assumed.)

Witkin assumed that the planar surface S contains a set of line elements, or "needles". Let β_i be the angle between line segment i and an axis in S aligned with the tilt direction. These line elements are projected onto the image I. Let α_i be the angle between the projected line segment and the x axis in I.

Witkin made the important observation that the β_i's are transformed to the α_i's in a way that depends systematically on the surface orientation (σ, τ). In orthographic projection, this transformation is given by

$$\alpha = \arctan(\frac{\tan \beta}{\cos \sigma}) + \tau \tag{1}$$

(See [12] for a detailed derivation). Qualitatively, this equation says that the more slant is increased, the more the projected needles will tend towards the direction perpendicular to the tilt direction.

The ML estimator is based on the following assumptions:

1. All needle directions are equally likely, i.e. each β_i is a sample from a uniform distribution
2. The needle directions are independent
3. The projection is orthographic

From these assumptions the probability density function $D(A \mid \sigma, \tau)$ for the sample set $A = \{\alpha_i\}_{i=1}^n$ can be computed [5]:

$$D(A \mid \sigma, \tau) = \frac{1}{\pi^n} \prod_{i=1}^{n} \frac{\cos \sigma}{\cos^2(\alpha_i - \tau) + \cos^2 \sigma \sin^2(\alpha_i - \tau)} \tag{2}$$

The maximum likelihood estimate of surface orientation is then defined as the pair $(\hat{\sigma}, \hat{\tau})$ which maximizes this probability density function.

Witkin actually used the "maximum a posteriori" (MAP) estimate, which is slightly different: it is the pair (σ, τ) that maximizes the probability density function $D(\sigma, \tau \mid A)$. This estimator requires knowledge of the prior probability distribution for surface orientation. In practice the difference between the two estimators is small, since the ML function and the MAP function only differ by a factor of $\sin\sigma$. We will henceforth discuss the ML rather than the MAP estimator.

The likelihood function depends in a non-linear way on each of the observed angles α_i, and to maximize it is therefore a non-trivial task. Iterative approaches have been suggested e.g. by Davis *et al* [5] and Blake and Marinos [1]. A related approach will be described in Section 5.

3 Statistics of directional data

The ML estimator is based on the *directional* statistics of oriented texture elements, and the analysis of such distributions poses some particular problems. Consider a set of undirected line segments in the plane, and let $\alpha \in [0, \pi)$ be the angle between a line segment and some reference direction. The fact that α and $\alpha + \pi$ represent the same direction means that conventional statistical concepts can lead to paradoxes; for example, the average of 1° and 179° should be 0° and not 90°.

Fortunately, this problem can be eliminated in a straightforward manner, by treating directional data as *distributions on the unit circle* rather than distributions on the line. With this technique, a quantity x with period L is represented by the point $(\cos 2\pi x/L, \sin 2\pi x/L)$. Distributions on the circle are used routinely in many branches of applied science. A comprehensive overview of the theory is given by Mardia [11], who also includes many examples from physics, astronomy, biology, geology, meteorology, geography, and other disciplines.

The most important characteristics of ordinary "distributions on the line" are the *mean* and *variance*, and similar measures can be defined for distributions on the circle.

Formally, let $F(\alpha)$ be a weight distribution on the interval $\alpha \in [0, \pi]$. As discussed above, it can equivalently be considered as a weight distribution on the unit circle by the mapping $\alpha \mapsto (\cos 2\alpha, \sin 2\alpha)$. The interpretation of $F(\alpha)$ is that $F(\alpha_2) - F(\alpha_1)$ specifies the weight in the interval $\alpha \in [\alpha_1, \alpha_2]$. Hence, we will always have $F(0) = 0$.

In the following we will always assume that $F(\alpha)$ is normalized, i.e., that $F(\pi) = 1$. The most fundamental descriptive measure of a weight distribution F on the circle is its *center of mass* $(\bar{C}, \bar{S})$, defined by

$$\begin{aligned} \bar{C} &= \int_0^\pi \cos 2\alpha \, dF(\alpha) \\ \bar{S} &= \int_0^\pi \sin 2\alpha \, dF(\alpha) \end{aligned} \tag{3}$$

In the case of an atomic distribution restricted to the directions $\{\alpha_i\}_{i=1}^n$ with the normalized weights $\{w_i\}_{i=1}^n$, the above expression is simplified to

$$\begin{aligned} \bar{C} &= \sum_{i=1}^n w_i \cos 2\alpha_i \\ \bar{S} &= \sum_{i=1}^n w_i \sin 2\alpha_i \end{aligned} \tag{4}$$

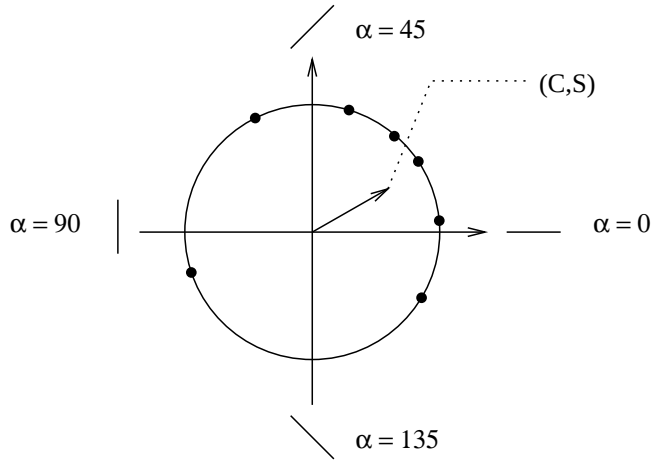

Figure 2: An atomic weight distribution on the circle and its center of mass.

It is easy to see that the center of mass will always lie inside or on the perimeter of the circle (see Figure 2 which exemplifies an atomic distribution). It is often useful to express the center of mass in polar coordinates $(Q, 2\psi)$:[1]

$$\begin{aligned} Q &= \sqrt{\bar{C}^2 + \bar{S}^2} \\ \psi &= \tfrac{1}{2} \arg(\bar{C}, \bar{S}) \end{aligned} \tag{5}$$

Hence, $Q \in [0, 1]$ is the distance from the center of the circle to the center of mass and 2ψ is the corresponding direction. The interpretation of Q and ψ is straightforward: ψ is the *mean direction*, and Q is a measure of *anisotropy*, i.e., how much the distribution is biased towards any particular direction. The quantity $1 - Q$ is often referred to as the *circular variance* of the distribution. It can be shown that $Q = 1$ if and only if the distribution is concentrated at a single point $\alpha = \alpha_0$ [11].

Note that ψ is undefined when $Q = 0$. This means that there is no particular mean direction—any direction would do equally well. We call such distributions *weakly isotropic*. This concept can also be applied to a finite sample of directions, in which case we say that the *sample* is weakly isotropic. The idea of a weakly isotropic sample is closely related to Witkin's ML estimator; this will be discussed in Section 5.

4 The MM estimator

The computational complexity of the ML estimator is a consequence of the fact that the likelihood function depends explicitly on each projected angle α_i. In this section we propose an alternative estimator, which has three attractive properties. Firstly, it only uses the directional statistics (Q, ψ) of the projected needles, instead of all the individual orientations. Secondly, there is a *closed-form expression* for the estimate $(\hat{\sigma}, \hat{\tau})$ as a function of (Q, ψ). Thirdly, the estimation problem is *decoupled*: the estimated slant $\hat{\sigma}$ only depends on Q, and the estimated tilt $\hat{\tau}$ only depends on ψ.

[1] Remember that the center of mass refers to 2α. We call the angle 2ψ so that we can relate ψ to α.

Formally, the estimator we propose is the *method of moments* (MM) applied to distributions on the unit circle. On the line the method of moments is dubious since the moments may not always exist, but the trigonometric moments $(\bar{C}, \bar{S})$ on the circle do not have this disadvantage. The MM estimates are consistent and asymptotically normal [11].

Assume as in Section 2 that n needle directions α_i have been observed in the image. Let each needle be given the weight $1/n$. The centroid $(\bar{C}, \bar{S})$ of this weight distribution is given by (4):

$$\begin{aligned} \bar{C} &= \frac{1}{n}\sum_{i=1}^{n} \cos 2\alpha_i \\ \bar{S} &= \frac{1}{n}\sum_{i=1}^{n} \sin 2\alpha_i \end{aligned}$$

Let

$$a(\sigma,\tau) = E(\cos 2\alpha \mid \sigma,\tau), \quad b(\sigma,\tau) = E(\sin 2\alpha \mid \sigma,\tau)$$

where $E(\cdot)$ denotes expected value. The MM estimates of σ and τ are the solution of

$$\bar{C} = a(\sigma,\tau), \quad \bar{S} = b(\sigma,\tau) \tag{6}$$

Hence, the MM estimator is based on the assumption that the observed centroid $(\bar{C}, \bar{S})$ is equal to its expected value.

We will now derive a closed-form expression for the MM estimate under the assumptions made in the derivation of the ML algorithm, i.e., that the β_i's are uniformly distributed and that the projection is orthographic. Making the substitution $\alpha' = \alpha - \tau$ in (1) we have

$$\tan\alpha' = \tan(\alpha - \tau) = \frac{\tan\beta}{\cos\sigma} \tag{7}$$

and

$$\begin{aligned} a &= E(\cos 2\alpha \mid \sigma,\tau) \\ &= E(\cos 2\alpha' \mid \sigma,\tau)\cos 2\tau - E(\sin 2\alpha' \mid \sigma,\tau)\sin 2\tau \\ &= a'\cos 2\tau - b'\sin 2\tau \\ b &= E(\sin 2\alpha \mid \sigma,\tau) \\ &= E(\sin 2\alpha' \mid \sigma,\tau)\cos 2\tau + E(\cos 2\alpha' \mid \sigma,\tau)\sin 2\tau \\ &= b'\cos 2\tau + a'\sin 2\tau \end{aligned}$$

where the definition of a' and b' is the obvious one. Using (7) to substitute for α' we obtain

$$\begin{aligned} a' &= E(\cos 2\alpha' \mid \sigma,\tau) \\ &= E\left(\frac{\cos^2\sigma - \tan^2\beta}{\cos^2\sigma + \tan^2\beta}\right) \\ &= E\left(\frac{\cos^2\sigma\cos^2\beta - \sin^2\beta}{\cos^2\sigma\cos^2\beta + \sin^2\beta}\right) \\ &= \int_0^{\pi} \frac{\cos^2\sigma\cos^2\beta - \sin^2\beta}{\cos^2\sigma\cos^2\beta + \sin^2\beta}\frac{1}{\pi}\,d\beta \end{aligned}$$

$$= -\frac{1-\cos\sigma}{1+\cos\sigma}$$

$$\begin{aligned} b' &= E(\sin 2\alpha' \mid \sigma,\tau) \\ &= E(\frac{2\cos\sigma\tan\beta}{\cos^2\sigma+\tan^2\beta}) \\ &= 2\cos\sigma E(\frac{\cos\beta\sin\beta}{\cos^2\sigma\cos^2\beta+\sin^2\beta}) \\ &= 2\cos\sigma\int_0^\pi \frac{\cos\beta\sin\beta}{\cos^2\sigma\cos^2\beta+\sin^2\beta})\frac{1}{\pi}\,d\beta \\ &= 0 \end{aligned}$$

where the details of the evaluation of the integrals have been omitted. Substituting this result into (6) we have

$$\bar{C} = -\frac{1-\cos\sigma}{1+\cos\sigma}\cos 2\tau \tag{8}$$

$$\bar{S} = -\frac{1-\cos\sigma}{1+\cos\sigma}\sin 2\tau \tag{9}$$

The MM estimate is obtained by solving for σ and τ, and we summarize the result as a proposition:

Proposition 1 (The MM estimator) *Let α_i, $i = 1\ldots n$, be the directions of independent oriented texture elements observed in the image. Under the same assumptions made in the derivation of the ML estimator, the MM estimator of surface orientation (σ,τ) is*

$$\sigma = \arccos\frac{1-Q}{1+Q} \tag{10}$$

$$\tau = \psi \pm \frac{\pi}{2} \pmod{2\pi} \tag{11}$$

where

$$Q = \sqrt{\bar{C}^2+\bar{S}^2}, \qquad \psi = \frac{1}{2}\arctan(\bar{S},\bar{C})$$

and

$$\begin{aligned} \bar{C} &= \frac{1}{n}\sum_{i=1}^{n}\cos 2\alpha_i \\ \bar{S} &= \frac{1}{n}\sum_{i=1}^{n}\sin 2\alpha_i \end{aligned}$$

Note that, as expected, the estimate of σ only depends on Q and the estimate of τ only depends on ψ.

5 Efficient computation of the ML estimate

In Section 6 we will demonstrate that the MM estimate usually provides an excellent approximation to the ML estimate. This fact can be exploited to design an efficient algorithm for iterative computation of the ML estimate.

Blake and Marinos [1] have shown that the maximum likelihood estimate makes isotropic a certain *second moment tensor* of the directions of the backprojected needles. This result can be given a natural interpretation in terms of the *weak isotropy* concept introduced in Section 3. Let $\alpha_i'(\sigma,\tau)$ be the orientation of a backprojected needle with orientation α_i in the image. Giving equal weight to all line segments, the center of mass of the directional distribution of the backprojected needles is then simply

$$\begin{aligned} \bar{C}'(\sigma,\tau) &= \frac{1}{n}\sum_{i=1}^{n}\cos 2\alpha_i' \\ \bar{S}'(\sigma,\tau) &= \frac{1}{n}\sum_{i=1}^{n}\sin 2\alpha_i' \end{aligned} \tag{12}$$

and the ML estimate is characterized by the fact that $\bar{C}' = \bar{S}' = 0$, i.e., that the set of backprojected needles is weakly isotropic. A direct proof (not using tensors) can be found in [6].

A standard technique for numerical solution of such systems of nonlinear equations is Newton-Raphson's method [3]. This technique has the benefit that the error decreases quadratically, provided that the estimate lies sufficiently close to the real root. An algorithm based on Newton-Raphson's method was suggested earlier by Davis *et al* [4], but they state that their algorithm often failed to converge, and it was therefore not used in the experimental results they report. In contrast, we have had no convergence problems with the Newton-Raphson method when using the MM estimate as an initial approximation.

6 Experimental results

In this section we demonstrate the performance of the MM estimator and compare it to that of the ML estimator, first on synthetic data and then on subwindows of a real gray-level image.

The MM and ML estimates were computed as explained previously. First, the directional statistics in polar form (Q,ψ) of the projected needles were computed, and the MM estimate was obtained using Proposition 1. The ML estimate was then computed using the iterative procedure described in the previous section. The iterations were terminated when the angle between two successive estimates of the surface normal became less than $0.05°$, which typically took two or three iterations. Of course, this very high accuracy is not meaningful in practice; other sources of uncertainty—such as errors in the texture element extraction—will usually have a much larger influence on the total estimation error.

6.1 Synthetic data

The first set of experiments was designed to allow a systematic comparison of the performance of the MM and ML estimators under controlled conditions.

We define the error ϵ of an estimate $(\hat{\sigma},\hat{\tau})$ as the angle between the associated surface normal and the true surface normal. The surface normal $\hat{\mathbf{n}}$ associated with the slant and tilt values (σ,τ) is

$$\hat{\mathbf{n}} = \begin{pmatrix} \sin\sigma\cos\tau \\ \sin\sigma\sin\tau \\ -\cos\sigma \end{pmatrix} \tag{13}$$

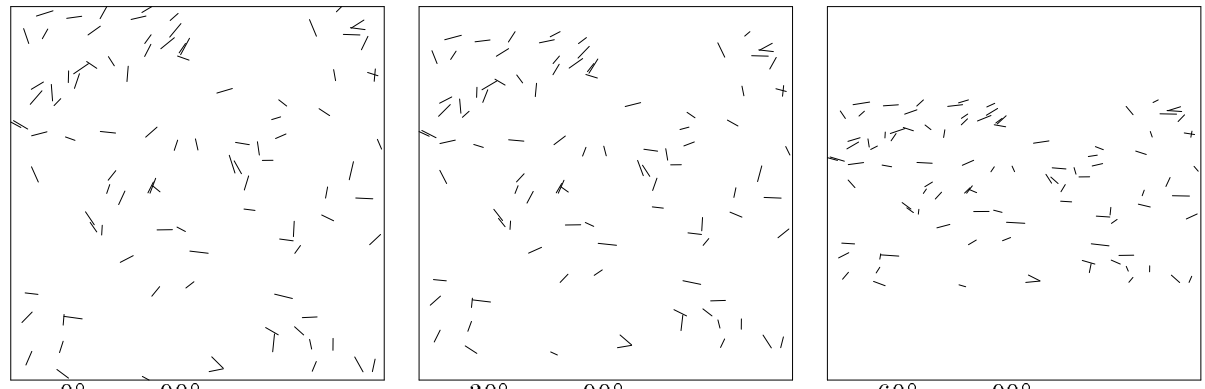

Figure 3: A synthetic texture viewed with three different values of slant.

Slant σ			Angles between surface normals								
	Mean est.		Mean			St. dev.			Max		
True	MM	ML	ϵ_{MM}	ϵ_{ML}	Δ	ϵ_{MM}	ϵ_{ML}	Δ	ϵ_{MM}	ϵ_{ML}	Δ
0	31.4	31.5	31.4	31.5	1.3	9.0	9.1	0.7	53.9	53.8	3.7
30	34.7	34.8	15.8	16.0	1.4	7.7	7.7	0.8	37.2	39.3	3.4
60	60.5	60.5	5.9	5.7	2.0	3.2	3.1	0.9	16.3	16.3	4.1

Table 1: Comparison of the MM and ML estimators; statistics from 100 trials. All values are given in degrees. The first three columns show the true slant, and the mean values of the MM and ML slant estimates. The remaining columns summarize the errors in the MM and ML estimates, and the difference between each pair of estimates: ϵ_{MM} is the angle between the true surface normal and the surface normal given by the MM estimate. ϵ_{ML} is the angle between the true surface normal and the surface normal given by the ML estimate. Δ is the angle between the surface normals corresponding to the MM and ML estimates respectively.

A set of 100 synthetic random textures was generated, each containing 100 line segments. The orientation of each segment was drawn from a uniform distribution on $(0, \pi)$. The positions and lengths of the line segments are irrelevant for the purpose of this experiment.

Each texture was projected orthographically from planes with slant 0°, 30°, and 60°. The tilt was 90° in all cases. An example is shown in Figure 3. The results of the experiment are summarized in Table 1. For each value of true slant we give the arithmetic mean of the MM and ML slant estimates, as well as the mean, standard deviation, and maximum of the surface normal angles ϵ_{MM}, ϵ_{ML}, and Δ (see the table caption for definitions).

The main conclusion of this experiment is that the difference Δ between the MM and ML estimates is very small compared to the differences ϵ_{MM} and ϵ_{ML} between each estimate and the true surface orientation. In other words, the MM and ML estimators have a strong tendency to err in the same direction. In fact, under the ideal conditions used in this experiment, there seems to be no significant difference between the performance of the two estimators.

It also worth pointing out that the arithmetic means of the estimated slant values as given in the second and third columns of Table 1 are generally *not* consistent estimators of

the true slant. This is readily appreciated by considering the case $\sigma = 0$, where any error in the estimated surface orientation causes slant to be overestimated. To obtain a single consistent slant estimate using all 100 images from each set, one should instead combine all line segments into a single image and then apply the MM and ML estimators. The slant estimates obtained this way, corresponding to the true slants 0°, 30°, and 60°, are 7.2°, 30.8°, and 60.3° for both the MM and ML estimators.

6.2 Natural images

In order to apply the MM or ML estimator to real gray-level images, one must first find a way of extracting independent needle-like texture elements from the image. This is obviously a very difficult segmentation problem, and a general solution for arbitrary textures does not seem feasible. As a compromise, one may ignore the independence assumption and simply use contour elements extracted from the image. Witkin [12] took this approach and suggested using the zero-crossings of the Laplacian of the Gaussian. Unfortunately, ignoring the independence assumption results in overestimation of slant [2, 6].

Furthermore, the assumption of orthographic projection is also violated whenever real images are used, which may or may not cause significant estimation errors depending on the field of view and the slant of the surfaces in the scene. However, since the aim of the present paper is to compare the MM and ML estimators which are both derived from the same statistical and geometric models, we will not attempt to compensate for errors due to violations of any of the model assumptions (but see [7] for an alternative approach based on perspective projection and piecewise smooth contours rather than independent needles.)

The needle extraction method used here is similar to Witkin's technique, but based instead on the *first* Gaussian-smoothed derivatives in the x and y directions (using a standard deviation equal to 0.5 pixels). The magnitude of this gradient is computed for each image point, followed by suppression of non-maxima in the direction of the gradient. An adaptive gradient magnitude threshold is then determined such that 10% of all pixels in the current region of interest remain. The direction perpendicular to the gradient at these points is then used as input to the estimators.

Figure 4 shows the results of applying the MM-ML technique to four subimages (with no overlap) of an outdoor scene. The similarity between the MM and ML estimators is remarkable; in three of the four windows the angle between the resulting surface normals was less than one degree. Starting from the direct MM estimate, two or three iterations were always sufficient to attain the predetermined accuracy of 0.05° in the ML estimate.

7 Conclusions

We have proposed a *direct* estimator for surface orientation, based on the method of moments (MM) applied to distributions on the unit circle. The MM estimator was derived under precisely the same assumptions as Witkin's ML estimator. The performance of the MM and ML estimators were compared for both synthetic data and a real gray-level image, and the difference was shown to be remarkably small.

We have also briefly described an efficient algorithm for computing the ML estimate. In this algorithm the MM estimate is used as an initial approximation in a standard Newton-Raphson iterative technique for solving a system of two non-linear equations. This MM-ML algorithm appears to compare favorably to previous techniques. It is obviously much less

Original image

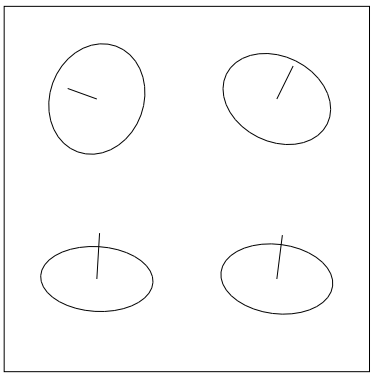

MM estimates

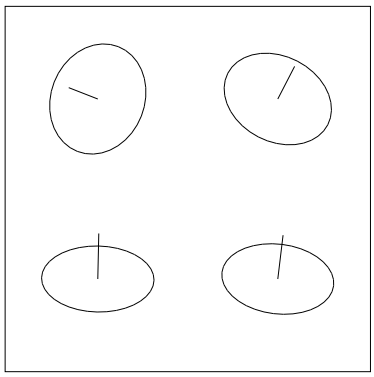

ML estimates

Window	Slant σ MM	Slant σ ML	Tilt τ MM	Tilt τ ML	Δ	Anisotropy Q Image	Anisotropy Q MM	Anisotropy Q ML	ML iterations
bot. left	54.8°	54.1°	86.6°	88.8°	1.90°	0.27	0.024	$4.3 \cdot 10^{-12}$	3
bot. right	51.9°	51.7°	82.8°	83.1°	0.33°	0.24	0.004	$1.2 \cdot 10^{-9}$	2
top left	33.4°	33.7°	160.1°	158.6°	0.85°	0.09	0.005	$5.7 \cdot 10^{-8}$	2
top right	40.9°	40.7°	63.7°	62.7°	0.68°	0.14	0.005	$2.0 \cdot 10^{-8}$	2

Figure 4: Empirical comparison of the MM and ML estimators using a real gray-level image. σ, τ, and Δ are given in degrees. Δ is the angle between the MM and ML estimates of the surface normal. The anisotropy measure Q (defined by (5)) is then listed for the needles extracted from the image, for the backprojection of the needles to the surface given by the ML estimate, and for the backprojection of the needles to the surface given by the iteratively computed approximation to the ML estimate (where the exact ML estimate has $Q = 0$). Finally, the rightmost column shows the number of iterations required to compute the ML estimate to within 0.05° starting from the MM estimate.

expensive and more accurate than Witkin's original exhaustive search [12]. It does not have the convergence problems reported by Davis *et al* [4]. Blake and Marinos [1] find the ML estimate by iterative computation of second moment tensors, and report a typical accuracy after one iteration of 1° for τ and 10° for σ, which is clearly inferior to the typical accuracy of the MM estimate. The rate of convergence of their scheme is somewhat difficult to judge, but it does not seem likely that it is higher than that of the MM-ML algorithm which has quadratic convergence.

As noted by many authors, the main drawback of the MM and ML approaches lies in the restrictive texture model, which requires independent texture elements to be identified in the image. Alternative methods [7, 10] based on piecewise smooth contours instead of independent elements have in fact eliminated this problem, but these approaches are deterministic rather than probabilistic. An approach combining the benefits of a probabilistic description with a more realistic texture model has yet to be found.

Acknowledgments

I thank Jan-Olof Eklundh for stimulating discussions and valuable advice. The support of the Swedish National Board for Industrial and Technical Development (NUTEK) is gratefully acknowledged. This work has been partially funded by the InSight project within

the ESPRIT BRA (Basic Research Action).

References

[1] A. Blake and C. Marinos, "Shape from texture: estimation, isotropy and moments", *J. of Artificial Intelligence*, vol. 45, pp. 323–380, 1990.

[2] M. Brady and A. Yuille, "An extremum principle for shape from contour", *IEEE Trans. Pattern Anal. and Machine Intell.*, vol. 6, pp. 288–301, 1984.

[3] G. Dahlquist and Å. Björk, *Numerical Methods*. Prentice-Hall, Englewood Cliffs, NJ, 1974.

[4] L.S. Davis, L. Janos, and S.M. Dunn, "Efficient recovery of shape from texture", Tech. Rep. TR-1133, Computer Vision Laboratory, U. of Maryland, May 1982.

[5] L.S. Davis, L. Janos, and S.M. Dunn, "Efficient recovery of shape from texture", *IEEE Trans. Pattern Anal. and Machine Intell.*, vol. 5, pp. 485–492, Sept. 1983.

[6] J. Gårding, *Shape from surface markings*. PhD thesis, Dept. of Numerical Analysis and Computing Science, Royal Institute of Technology, Stockholm, May 1991.

[7] J. Gårding, "Shape from texture and contour by weak isotropy", *J. of Artificial Intelligence*, 1992. (In press).

[8] J. Gårding, "Shape from texture for smooth curved surfaces in perspective projection", *J. of Mathematical Imaging and Vision*, 1992. (In press).

[9] J. Gibson, *The Perception of the Visual World*. Houghton Mifflin, Boston, 1950.

[10] K. Kanatani, "Detection of surface orientation and motion from texture by a stereological technique", *J. of Artificial Intelligence*, vol. 23, pp. 213–237, 1984.

[11] K.V. Mardia, *Statistics of Directional Data*. Academic Press, London, 1972.

[12] A.P. Witkin, "Recovering surface shape and orientation from texture", *J. of Artificial Intelligence*, vol. 17, pp. 17–45, 1981.